

Contrast image correction method

Raimondo Schettini
Francesca Gasparini
Silvia Corchs
Fabrizio Marini

Università degli Studi di Milano-Bicocca
Dipartimento di Informatica, Sistemistica e Comunicazione
Viale Sarca 336
20126 Milano, Italy
E-mail: silvia.corchs@disco.unimib.it

Alessandro Capra
Alfio Castorina

STMicroelectronics Catania
Advanced System Technology—Catania Lab
Italy

Abstract. A method for contrast enhancement is proposed. The algorithm is based on a local and image-dependent exponential correction. The technique aims to correct images that simultaneously present overexposed and underexposed regions. To prevent halo artifacts, the bilateral filter is used as the mask of the exponential correction. Depending on the characteristics of the image (piloted by histogram analysis), an automated parameter-tuning step is introduced, followed by stretching, clipping, and saturation preserving treatments. Comparisons with other contrast enhancement techniques are presented. The Mean Opinion Score (MOS) experiment on grayscale images gives the greatest preference score for our algorithm. © 2010 SPIE and IS&T. [DOI: 10.1117/1.3386681]

1 Introduction

Let us consider a scene of a room illuminated by a window that looks out on a sunlit landscape. A human observer inside the room can easily see individual objects in the room, as well as features in the outdoor landscape. This is because the eye adapts locally as we scan the different regions of the scene. If we attempt to photograph our view, the result could be disappointing: either the window is overexposed and we cannot see outside, or the interior of the room is underexposed and looks black.

Several methods for adjusting image contrast have been developed in the field of image processing. In general, we can discriminate between two classes of contrast corrections: global corrections and local corrections. Global contrast corrections can produce disappointing results when both shadow and highlight details have to be adjusted simultaneously. On the other hand, the advantage of the local contrast corrections is that they provide a method to map one input value to many different output values, depending on the values of the neighboring pixels and allowing in this

way for simultaneous shadow and highlight adjustments. Of the global contrast enhancement techniques, we found gamma correction and histogram equalization to be the most common. Gamma correction is a simple exponential correction and is common in most codes for image processing. Histogram equalization techniques have also been used by different authors. Based on the image's original gray-level distribution, the image's histogram is reshaped into a different one with uniform distribution property in order to increase the contrast. Numerous improvements have also been made to simple equalization by incorporating models of perception.¹⁻³

Different algorithms for local contrast correction have also been proposed. Moroney⁴ uses nonlinear masking in order to perform local contrast correction. This correction can simultaneously lighten shadows and darken highlights, and it is based on a simple pixel-wise gamma correction of the input data. However, one of the limitations of the Moroney's algorithm (common also to other local corrections) is the introduction of "halo" artifacts (due to the smoothing across scene boundaries) and also the shrinking of the dynamic range of the scene. The adaptive histogram equalization (AHE) methods use local image information to enhance the image. In Ref. 5, several adaptive (AHE) techniques are reviewed and compared. The author also proposed a new AHE method based on a "modified cumulation function" that introduces two parameters. Arici *et al.*⁶ presented a general framework based on histogram equalization where contrast enhancement is posed as an optimization problem that minimizes a cost function. The authors also introduce penalty terms into the optimization problem in order to handle noise robustness and black/white stretching. Both these methods can achieve different levels of contrast enhancement, from histogram equalization to no contrast enhancement, through the use of different adaptive parameters. Depending on the image content, these parameters have to be manually set.

Paper 09135R received Jul. 28, 2009; revised manuscript received Jan. 11, 2010; accepted for publication Mar. 2, 2010; published online Apr. 15, 2010.

1017-9909/2010/19(2)/023005/11/\$25.00 © 2010 SPIE and IS&T.

The retinex model introduced by Land and McCann⁷ has been applied for many image processing tasks and in particular for image enhancement. This model aims to predict the sensory response of lightness. The fundamental concept behind retinex computation of lightness at a given image pixel is the comparison of the pixel's value to that of other pixels, and the main difference between the different retinex algorithms is the way in which the other comparison pixels are chosen, including the order in which they are chosen. The original way of defining comparisons is by following a path, or set of paths, from pixel to neighboring pixel through the image. Jobson *et al.*⁸ and Rahman *et al.*^{9–11} developed the retinex concept into a full-scale automatic image enhancement algorithm. Their method, called multiscale retinex with color restoration (MSRCR), combines color constancy with local contrast/lightness enhancement to transform digital images into renditions that approach the realism of direct scene observation. A different multiresolution approach for contrast enhancement is presented by Starck *et al.*¹² Using curvelet transform, the authors address the multiscale enhancement problem and apply their curvelet-based enhancement technique to edge detection and segmentation.

Rizzi *et al.*¹³ presented an algorithm for unsupervised enhancement of digital images with simultaneous global and local effects, called automatic color equalization (ACE). Inspired by some adaptation mechanisms of human vision, ACE realizes a local filtering effect by taking into account the color spatial distribution in the image. ACE has proven to achieve an effective color constant correction and a satisfactory tone equalization performing simultaneously global and local image corrections. However, the computational cost of the algorithm is very high. Fairchild and Johnson¹⁴ formulated a model called the image color appearance model (iCAM). The objective in formulating iCAM was to provide traditional color appearance capabilities, spatial vision attributes and color difference metrics in a simple model for practical applications such as high-dynamic-range tone mapping.

Rendering high-dynamic-range images (HDRIs) on low-contrast media, a process known as tone mapping, is also related to the problem of contrast enhancement.

Photographers use *dodging and burning* to locally adjust print exposure in a dark room, inspiring an early paper by Chiu *et al.*¹⁵ that constructs a locally varying attenuation factor by repeatedly clipping and low-pass filtering the scene. Their method works well in smoothly shaded regions. Larson *et al.*¹⁶ presented a tone reproduction operator that preserves visibility in high-dynamic-range scenes. They introduced a new histogram adjustment technique, based on the population of local adaptation luminance in a scene. Tumblin and Turk¹⁷ devised a hierarchy that closely follows artistic methods for scene renderings. Each level of hierarchy is made from a simplified version of the original scene consisting of sharp boundaries and smooth shadings. They named the sharpening and smoothing method low-curvature image simplifiers (LCIS). The technique was shown to be effective to convert high-contrast scenes to low-contrast, highly detailed display images. A survey of early methods and algorithms able to deal with high-dynamic-range images is presented in Battiato *et al.*¹⁸ More recently, other authors have explored similar ideas—for ex-

ample, Meylan and Süssstrunk¹⁹ proposed a method to render high-dynamic-range images based on the center-surround retinex model. Their method uses an adaptive filter, whose shape follows the image's high-contrast edges, thus reducing halo artifacts common to other methods. Another well-known tone mapping approach is the fast bilateral filtering of Durand and Dorsey.²⁰ Their method is based on anisotropic diffusion to enhance boundaries while smoothing nonsignificant intensity variations. This strategy is similar to the one of Tumblin and Turk,¹⁷ but the use of the bilateral filter enables a speed-up compared to the partial derivative filter proposed by Tumblin and Turk, as well as enhanced stability. Pattanik and colleagues²¹ developed a computational model of adaptation spatial vision for tone reproduction. Their model is based on a multiscale representation of pattern, luminance, and color processing in the human visual system.

In our work, a local contrast correction is developed starting from Moroney's technique, where instead of the Gaussian filter, which produces the halo artifacts, the *bilateral filter* of Tomasi and Manduchi²² is used. Bilateral filtering smoothes images while preserving edges by means of a nonlinear combination of nearby image values. The bilateral filter combines gray levels or colors based on both their geometric closeness and their photometric similarity and prefers near values to distant values in both spatial and intensity domains. We also introduce here an image dependency to tune the strength of the correction with a parameter automatically evaluated from the global statistics of the image. Last, in order to improve the overall image enhancement, we introduce a histogram clipping procedure, also based on the image properties, automatically piloted by the histogram analysis, and an algorithm for color saturation gain. Preliminary results of this work have been presented in Ref. 23.

The paper is organized as follows. In Sec. 2, our algorithm is presented. In Sec. 3, we compare and discuss its performance with respect to other image enhancement methods available in the literature. A reliable way of assessing the quality of an image is by subjective evaluation. Therefore, a psychovisual test (Mean Opinion Score, or MOS) is performed to evaluate the quality of the correction. Last, Sec. 4 summarizes the conclusions.

2 Local Contrast Correction (LCC) Method

2.1 Local Exponential Correction in LCC

The method we propose for contrast enhancement is based on a local and image-dependent exponential correction. The simpler exponential correction, better known as *gamma correction*, is common in most codes for image processing and consists of elaborating the input image through a constant power function, with exponent γ . Let us assume for simplicity a gray image $I(i, j)$, of 8-bit range. The gamma correction transforms each pixel $I(i, j)$ of the input image into the output $O(i, j)$, according to the following rule:

$$O(i, j) = 255 \left[\frac{I(i, j)}{255} \right]^\gamma, \quad (1)$$

where γ is a positive number that usually varies between 0 and 3. This correction gives good results for totally underexposed or overexposed images. However, when both un-



Fig. 1 (a) Original image with simultaneous underexposed and overexposed regions. (b) Gamma correction with $\gamma=0.35$.

derexposed and overexposed regions are simultaneously present in an image, this correction is not satisfactory. In the image presented in Fig. 1 (left), the region of the window is well illuminated, whereas the rest of the photo is too dark to see the details. Applying gamma correction (with $\gamma=0.35$), the underexposed regions will become lighter as desired (making noticeable the details), but the central region of the photo will be overexposed, as seen in Fig. 1 (right).

The extension of Eq. (1) to a color image is straightforward, applying the rule to each of the components in the RGB space or only to the luminance Y in the YCbCr space. In what follows, we continue considering the case of a gray image. For the case of an image that has only certain regions with the correct illumination and other regions that are not well exposed, a local correction will be needed that allows for simultaneous shadow and highlight adjustments. As we are interested in a local correction, the exponent of the gamma correction will not be a constant but instead will be chosen as a function that depends on the point (i, j) to be corrected and on its neighboring pixels $N(i, j)$. Equation (1) thus becomes:

$$O(i, j) = 255 \left[\frac{I(i, j)}{255} \right]^{\gamma_{[i, j, N(i, j)]}} \quad (2)$$

Moroney⁴ suggested the following expression for the exponent:

$$\gamma_{[i, j, N(i, j)]} = 2^{[128 - \text{mask}(i, j)/128]}, \quad (3)$$

where $\text{mask}(i, j)$ is an inverted Gaussian low-pass filtered version of the intensity of the input image. Mask values greater than 128, corresponding to dark pixels with dark neighbors in the original image, will give rise to exponents γ smaller than 1, and therefore, from Eq. (2), an increase of the luminance will be observed. Values smaller than 128, corresponding to bright pixels with bright neighbors in the original image, will result in exponents γ greater than 1 and a decrease of the luminance. Mask values equal to 128 will produce an exponent equal to one, and no modification of the original input is obtained. The greater the distance from the mean value 128, the stronger the correction. We note that white and black pixels, as in the gamma correction, remain unaltered independently of the value of the exponent. In this work, Eq. (3) becomes:

$$\gamma_{[i, j, N(i, j)]} = \alpha^{[128 - \text{BFmask}(i, j)/128]}, \quad (4)$$

where $\text{BFmask}(i, j)$ is an inverted low-pass version of the intensity of the input image, filtered with a bilateral filter,²² and α is a parameter depending on the image properties. The creation of the mask and the choice of the parameter are extensively reported in the following sections.

2.2 Bilateral Filter in LCC

The Gaussian low-pass filtering computes a weighted average of pixel values in the neighborhood, in which the weights decrease with distance from the center. The assumption is that near pixels are likely to have similar values, and it is therefore appropriate to average them together. However, the assumption of slow spatial variations fails at edges, which are consequently blurred by low-pass filtering. In order to avoid averaging across edges, while still averaging within smooth regions, Tomasi and Manduchi²² presented the bilateral filter. Their idea was to do in the intensity range of an image what traditional filters do in its spatial domain. Two pixels can be close to one another—that is, occupy nearby spatial location—or they can be similar to one another—that is, have nearby values. The goal of using the bilateral filter to calculate the mask in Eq. (4) instead of the Gaussian filter proposed by Moroney is to decrease the halo effects that appear on certain images when only the spatial Gaussian filter is used. In particular, regions with high-intensity gradients are candidates to show the halo effect. One of the principal characteristics of the bilateral filter is to smooth images while preserving edges. Therefore, we expect the halo effect to decrease. The LCC algorithm we propose is a local exponential correction, applied to the intensity, as follows:

$$O(i, j) = 255 \left[\frac{I(i, j)}{255} \right]^{\alpha^{[128 - \text{BFmask}(i, j)/128]}} \quad (5)$$

The $\text{BFmask}(i, j)$ is defined over a window of size $(2K + 1) \times (2K + 1)$ and is given by the bifiltered image of the inverted version of the input $I_{\text{inv}}(i, j) = 255 - I(i, j)$:

$$\begin{aligned} \text{BFmask}(i, j) = & \frac{1}{k(i, j)} \sum_{p=i-K}^{i+K} \sum_{q=j-K}^{j+K} \\ & \times \exp \left\{ -\frac{1}{2\sigma_1^2} [(i-p)^2 + (j-q)^2] \right\} \\ & \times \exp \left\{ -\frac{1}{2\sigma_2^2} [I_{\text{inv}}(i, j) - I_{\text{inv}}(p, q)]^2 \right\} \\ & \times I_{\text{inv}}(p, q), \end{aligned} \quad (6)$$

where $k(i, j)$ is the normalization factor given by:

$$\begin{aligned} k(i, j) = & \sum_{p=i-K}^{i+K} \sum_{q=j-K}^{j+K} \exp \left\{ -\frac{1}{2\sigma_1^2} [(i-p)^2 + (j-q)^2] \right\} \\ & \times \exp \left\{ -\frac{1}{2\sigma_2^2} [I_{\text{inv}}(i, j) - I_{\text{inv}}(p, q)]^2 \right\}. \end{aligned} \quad (7)$$

In Eqs. (6) and (7), σ_1 is the standard deviation of the Gaussian function in the spatial domain, and σ_2 is the stan-



Fig. 2 Original image to be elaborated. Dimension: 511×341 .

standard deviation of the Gaussian function in the intensity domain. The parameter σ_1 is based on the desired amount of low-pass filtering. A large σ_1 blurs more—that is, combines values from more distant image locations. Similarly, σ_2 is set to achieve the desired amount of combination of pixel values. As σ_2 increases, the bilateral filter approaches the Gaussian low-pass filter. The dimension K of the window depends on the shape of the spatial Gaussian, through the following relation:

$$K = \lfloor 2.5 \times \sigma_1 \rfloor, \quad (8)$$

where $\lfloor \cdot \rfloor$ indicates “the integer part of.” If σ_1 is too high, the image results are too blurred, the exponent tends to a constant, and Eq. (5) tends to the simple gamma correction of Eq. (1). Otherwise, if the window is too small, the image is not blurred, and the correction does not take into account the local properties of the image.

In Fig. 2, an image is presented that shows a high-intensity gradient and thus is a candidate to represent the *halo effect*. The LCC output (with $\alpha=2$) and the corresponding bifilter mask are shown in Fig. 3 (left and right, respectively). The Moroney correction and the corresponding spatial Gaussian mask are shown in Fig. 4 (left and right, respectively). Comparing these two figures, we observe that the halo artifacts present in Fig. 4 are significantly reduced in Fig. 3. Different authors have followed the ideas of Tomasi and Manduchi, and in particular, Durand and Dorsey²⁰ provided a theoretical framework for bilateral filtering and also accelerated the method using a piecewise-linear approximation in the intensity domain and subsampling in the spatial domain. A fast approximation of the bilateral filter using a signal processing approach has

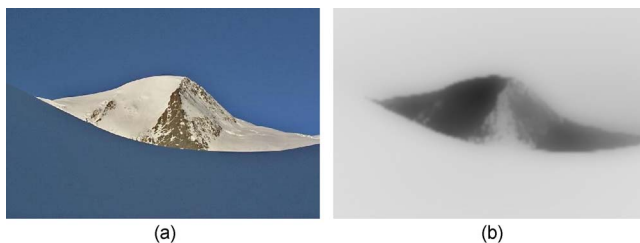


Fig. 3 (a) LCC output of Fig. 2. (b) Bilateral filtered mask used.

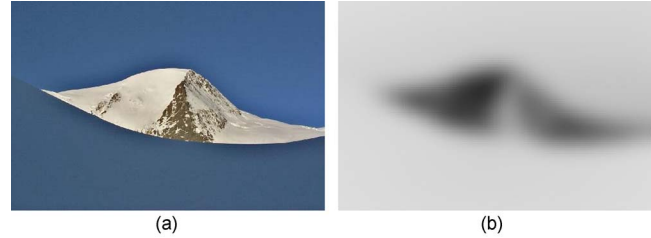


Fig. 4 (a) Moroney correction of Fig. 2. (b) Gaussian mask used.

been presented by Paris and Durand.²⁴ In our work, in order to make the bilinear filter algorithm faster, the spatial Gaussian in Eq. (6) is simply replaced by a box filter of dimension $3 \times \sigma_1$. The elaborated images do not show important differences, and the times are greatly reduced (by a factor of 7 in the case of Fig. 2).

2.3 α Parameter Optimization

In this section, we evaluate the more convenient value for α in Eq. (5) in the elaboration of a given image. In fact, it would be preferable to perform different contrast corrections depending on the characteristics of the single shot. For low-contrast images, where a stronger correction is needed, α should be high, say between 2 and 3, while for better contrasted images, α should diminish toward 1, which corresponds to no correction.

In order to develop an automatic tool to be applied to every image, a formulation of an estimated value of α is needed. Let us rewrite Eq. (5) in terms of expected values:

$$E[O(i,j)] = 255 \times E \left\{ \left[\frac{I(i,j)}{255} \right]^{\alpha^{[128-BFmask(i,j)/128]}} \right\}, \quad (9)$$

where E indicates expected value.

Starting from the Moroney formula [Eq. (3)], where the threshold for the mask inversion was set equal to 128, we set the mean value of a gray image equal to 128. Within this assumption, Eq. (9) becomes:

$$E[O(i,j)] = 255 \times E \left\{ \left[\frac{I(i,j)}{255} \right]^{\alpha^{[128-BFmask(i,j)/128]}} \right\}, \quad (10)$$

$$= 128.$$

As we know that $0 \leq \text{mask} \leq 255$, we can consider the two extreme conditions, and from Eq. (10), we will have the following two estimated values of α :

$$\alpha \cong \frac{\ln(\bar{I}/255)}{\ln(0.5)} \quad \text{when } BFmask = 255, \quad (11)$$

$$\alpha \cong \frac{\ln(0.5)}{\ln(\bar{I}/255)} \quad \text{when } BFmask = 0, \quad (12)$$

where \bar{I} is the estimated value or mean value of the intensity of the input image. If $\bar{I} < 128$, that means a dark image, mask values are toward 255, because it is associated with the negative of the intensity image, and thus Eq. (11) can be



Fig. 5 (a) Original image; dimension 320×240 . (b) LCC output with $\alpha=1.5$. (c) LCC output with $\alpha=2$. (d) LCC output with $\alpha=2.6$.

used for the estimation of α . Otherwise, if $\bar{I} > 128$ —that is, a bright image— α can be estimated with Eq. (12). The parameter α given by Eqs. (11) and (12) could be considered as a criterion to decide whether it is valid to apply the contrast enhancement method to the original image. That is, if α is close to one ($\alpha < 1.2$), we could argue that the original image does not need to be elaborated. As an example, we show in Fig. 5 an original dark photo and the corresponding elaborated LCC images for different values of the α parameter. The corresponding value of α in this case is evaluated from Eq. (11), and is equal to 2.6.

The entire enhancement procedure of our method is organized as a chain of algorithms, as indicated in Fig. 6. In the following sections, we explain the remaining modules corresponding to stretching, clipping, and color saturation.

2.4 Contrast Enhancement Chain: Stretching, Clipping, and Saturation Gain in LCC

2.4.1 Stretching and clipping

From a deeper analysis of the intensity histogram before and after the local correction proposed, we find that despite a better occupation of the gray levels, the overall contrast enhancement is not satisfying. Also, especially for low-quality images with compression artifacts, the noise in the darker zones is enhanced. These effects that make the processed image grayish are intrinsic in the mathematic formulation of Eq. (5) adopted for the local correction. To overcome this undesirable loss in the image quality, a further step of contrast enhancement, consisting of a stretching and clipping procedure, and an algorithm to increase the saturation are introduced in this section. The main characteristic of the contrast procedure we propose is that it is image dependent: stretching and thus clipping are piloted by the image histogram properties and are not fixed *a priori*. To determine the strength of the stretching and thus the number of bins to be clipped, it is considered how the darker regions occupy the intensity histogram before and after the LCC algorithm. The idea is that pixels belonging to a dark

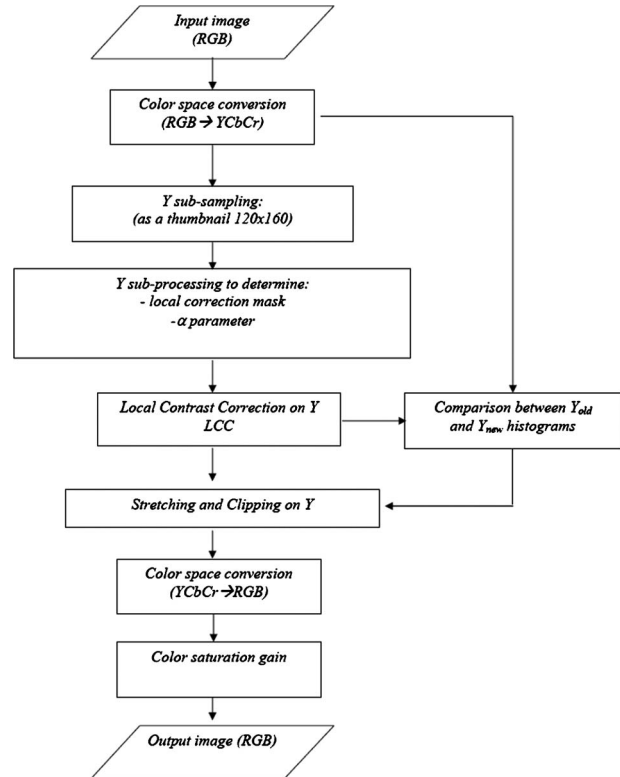


Fig. 6 Flowchart of the local contrast correction method proposed here.

area, such as a dark object, that usually occupy a narrow and peaked group of bins at the beginning of the intensity histogram will populate more or less the same bins after a contrast enhancement algorithm. On the other hand, pixels of an underexposed background that create a more spread histogram peak after the same algorithm must populate an even more widespread region of the histogram. To evaluate how these dark pixels are distributed, the algorithm proceeds as follows:

1. The RGB input image is converted to the YCbCr space. (This space is chosen because it is common in the case of JPEG compression, but other spaces where the luminance and the chrominance components are separated can be adopted.)
2. The percentage of the dark pixels in the image is computed. {A pixel is considered dark if its luminance Y is less than 35 and its chroma radius $[(Cb - 128)^2 + (Cr - 128)^2]^{1/2}$ is less than 20.}
3. If there are dark pixels, the number of stretched bins, b_{str} , is evaluated as the difference between the bin corresponding to the 30% of dark pixels in the cumulative histogram of the LCC output intensity, $b_{output30\%}$, and the bin, $b_{input30\%}$, corresponding to the same percentage in the cumulative histogram of the input intensity: $b_{str} = b_{output30\%} - b_{input30\%}$. In the case of dark regions that must be recovered, this percentage of pixels, which experience has suggested be set at 30%, generally falls in the first bins, under a narrow peak of the histogram, together with the rest of the dark pixels, and thus most of these

pixels are repositioned at almost the initial values. In the case of underexposed regions, however, the same percentage generally falls under a more widespread peak, and thus only part of the dark pixels are recovered.

4. If there are no dark pixels, the stretching is done to obtain a clipping of 0.2% of the darker pixels.
5. In any case, the maximum number of bins to be clipped is set to 50.

For the brighter pixels, the stretching is done to obtain a clipping of the 0.2%, with a maximum of 50 bins.

2.4.2 Color saturation

To minimize the change of the color saturation between the input and the output images, the following formulation is applied to the RGB channels, as suggested by Sakaue *et al.*²⁵ The transformed values R' , G' , B' are obtained as follows:

$$\begin{cases} R' = \frac{1}{2} \left[\frac{Y'}{Y} (R + Y) + R - Y \right] \\ G' = \frac{1}{2} \left[\frac{Y'}{Y} (G + Y) + G - Y \right] \\ B' = \frac{1}{2} \left[\frac{Y'}{Y} (B + Y) + B - Y \right] \end{cases}, \quad (13)$$

where Y' is the corrected luminance obtained after the (LCC+clipping) correction module, as indicated in the previous section.

3 Results and Discussion

In this section, we first present the results obtained when applying the LCC algorithm to two different kinds of images, and we show how the modules of stretching, clipping, and saturation further improve the correction depending on the image characteristics. In the second part of the results, the whole algorithm (LCC+clipping+saturation) is applied to different images and the results are compared with other image enhancement techniques.

In Fig. 7, a photo is shown where the darker part of the histogram (first 50 bins) corresponds to a dark region of the scene that we want to enhance. On the other hand, in Fig. 8, the dark areas (first 30 bins) are black regions of the image that we want to preserve (The black clothing). After applying the LCC module to Figs. 7 and 8, the new histograms are more widespread than the original but are moved and concentrated around the middle values of the range. Equation (5) applied to both images has the same effect of making these dark regions too bright. Moreover, the LCC corrected images show desaturated colors (middle row of Figs. 7 and 8). The next step of histogram stretching and clipping is different for these two figures. For Fig. 7, it is necessary to recover only partially the dark pixels, while for Fig. 8, all the dark pixels of the clothing must be recovered. In the bottom row of Figs. 7 and 8, the final elaborated images (LCC+clipping+saturation) and their corresponding histograms are shown. A correct redistribution of the histogram is obtained, and a good contrast correction is observed in both images (bottom row of Figs. 7 and 8).

As already mentioned, a great variety of algorithms for image enhancement are available in the literature. We recall that our method is essentially a contrast correction one, and we have considered only a module for color saturation at the end of the chain (as indicated in Sec. 2.4.2). In order to compare our algorithm's performance with some other methods, we first concentrate on the case of grayscale images. Figures 9 and 10 show two example input images and the results applying our method, the Moroney correction and the retinex method. This last one has been evaluated within its Frankle-McCann version, where four iterations have been used for the calculations.²⁶ Retinex and our method increase very well both the global and local contrasts, highlighting details that were hidden in the original image. However, we observe that the retinex results present an overenhancement effect, and we could consider our correction as a more natural one. The Moroney correction is globally darker with respect to the other results. Experimental results for other test grayscale images have shown similar tendencies.

3.1 Quality Assessment

The improvement in images after enhancement is often very difficult to measure. To date, no objective criteria to assess image enhancement capable of giving a meaningful result for every image exist in the literature. Full reference-quality assessment metrics cannot be applied, since these methods evaluate the departure of the output image with respect to an original one that is supposed to be free of distortions. In our present case of contrast enhancement, no such original "distortion-free" images exist, and the elaborated images should be an enhanced version of the input.

There exist some objective metrics in the literature that aim to estimate brightness and contrast in the image, such as entropy (H), absolute mean brightness error (AMBE), and measure of enhancement (EME).²⁷⁻²⁹ AMBE is the absolute difference between input and output mean, and EME approximates an average contrast in the image by dividing the image into nonoverlapping blocks, defining a measure based on minimum and maximum intensity values in each block and averaging them.

Absolute values of these metrics (H, AMBE, and EME) should be carefully analyzed, since they do not necessarily correlate with an improvement of image quality in terms of contrast enhancement. Let us note that, within this context, we are implicitly associating the image quality concept to the naturalness of the image. For example, with respect to the use of the EME metric, high values of EME should indicate regions with high local contrast, while EME values of nearly zero should correspond to homogenous regions. If an algorithm introduces noise in such homogenous regions, a higher EME value will be obtained, and this is certainly not in correspondence with an image quality improvement, as can be seen in the example shown in Fig. 11, where for the retinex processing, noise is amplified and the corresponding EME value equals 31.70. This value is higher than that corresponding to the other two algorithms compared here ($EME_{Identity}=25.09$, $EME_{LCC}=18.09$, $EME_{Moroney}=23.76$).

AMBE represents the distance from mean brightness of the original. In an enhancement procedure, we do not always want to preserve the original brightness. In fact, pre-

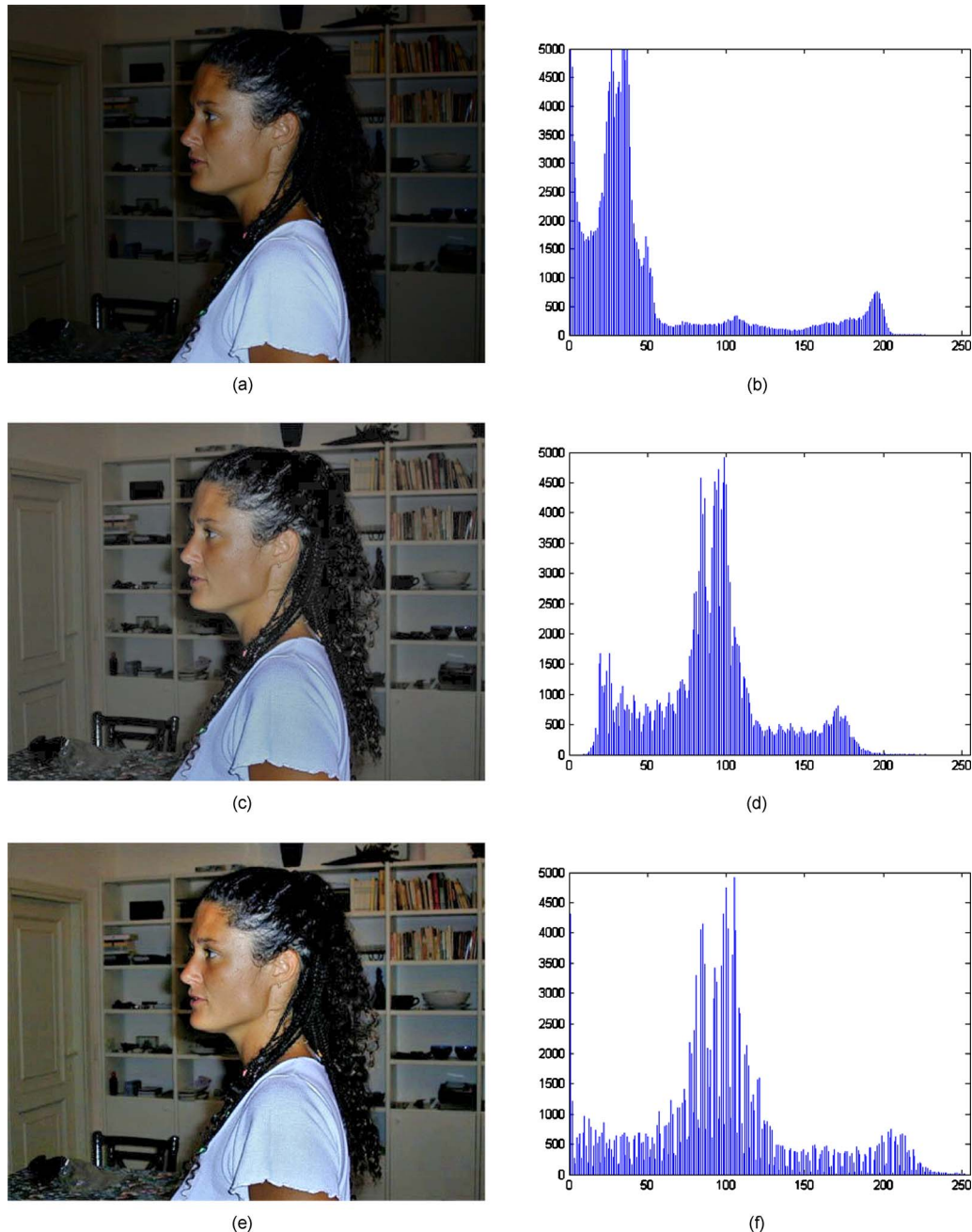


Fig. 7 (a) Original image. (b) Histogram of original image. In this case, the wide dark peak at the beginning of the histogram corresponds to the background (see text). (c) LCC output with $\alpha=2.5$. (d) Histogram of LCC output with $\alpha=2.5$. (e) Final elaborated image; LCC+clipping+saturation. (f) Histogram of final elaborated image.

serving the original brightness does not always mean preserving the natural look of the image. If the original images are strongly underexposed and/or overexposed, we expect a high AMBE value, indicating that the quality could have been improved. For example, our LCC correction applied to the image shown in Fig. 7 gives an AMBE value of 51.22. On the other hand, in the case of correctly exposed images or night photos, we expect our algorithm not to significantly modify the mean brightness. (See values of the metric for Fig. 11: $AMBE_{LCC}=18.89$, $AMBE_{Moroney}=23.86$, $AMBE_{Retinex}=48.58$.)

With respect to the entropy values, high values of H indicate a better occupation of all intensity levels. This will be associated with a visually pleasing image if the acquisition conditions were reasonably well balanced. Starting from images with sharply peaked histograms (underexposed and/or overexposed or night images), obtaining a flat histogram could increase noise. (See values of the metric for Fig. 11: $H_{identity}=5.86$, $H_{LCC}=6.01$, $H_{Moroney}=6.58$, $H_{Retinex}=7.61$.) Thus, the higher value of H (ideal flat histogram) does not always represent a visually pleasing image.

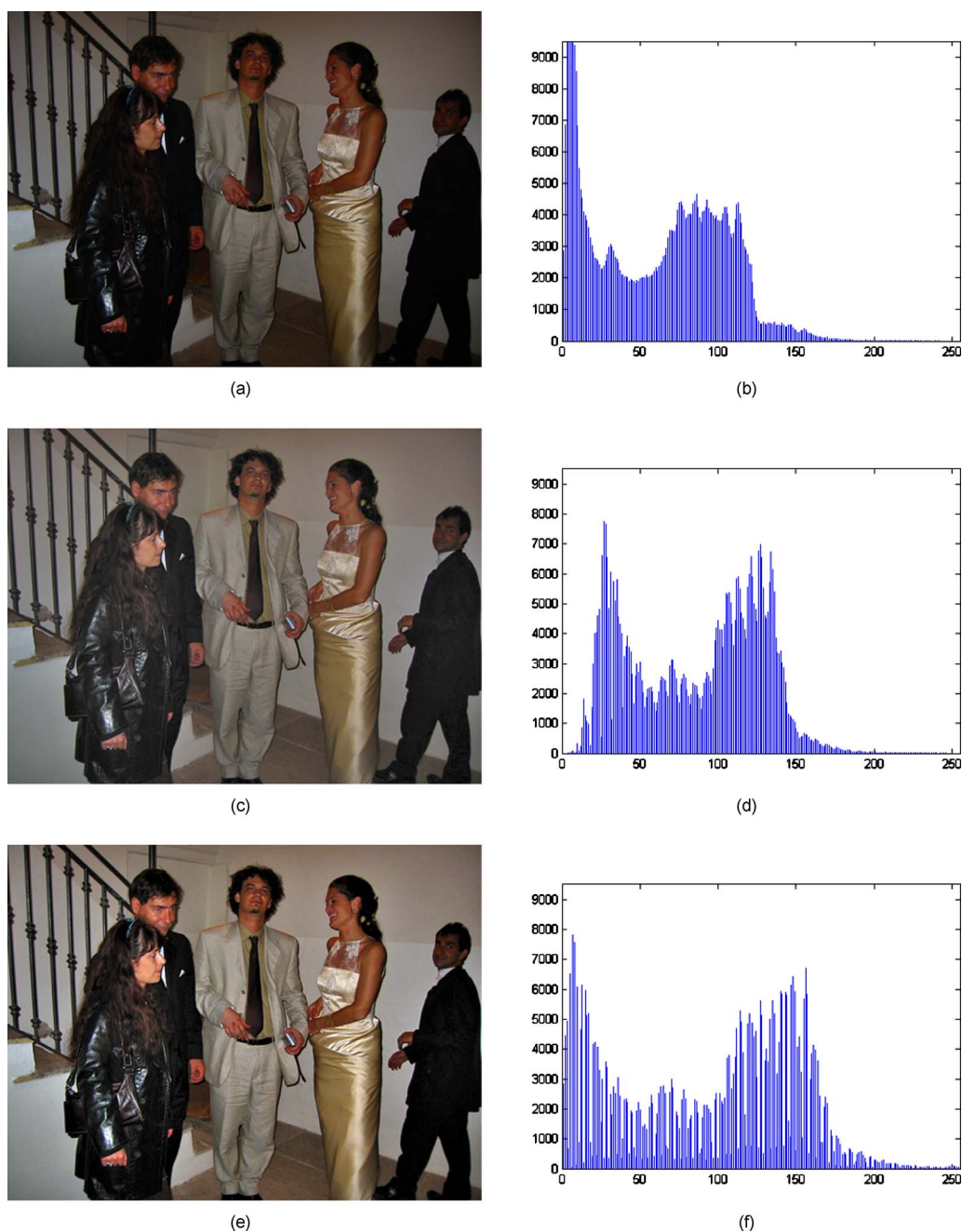


Fig. 8 (a) Original image. (b) Histogram of original image. In this case, the narrow dark peak at the beginning of the histogram is due to the black suits present in the photo (see text). (c) LCC output. (d) Histogram of LCC output. (e) Final elaborated images; LCC+clipping+saturation. (f) Histogram of final elaborated image.

Similar conclusions have been pointed out by Arici *et al.*,⁶ while evaluating the performance of their method with the same metrics.

Given all the considerations cited earlier about the objective metrics, we note that a reliable way of assessing the quality of an image is by subjective evaluation. Therefore, we have implemented the Mean Opinion Score (MOS) test to evaluate the performance of our algorithm and compare it with Moroney and retinex.

The MOS test, using paired comparison, was implemented for 10 images (indoor, outdoor, daylight, night, por-

trait) presenting underexposed and/or overexposed regions and 12 viewers. The preference score index is calculated for each of the preceding methods, and the greatest one (0.79) is obtained for our approach, agreeing with our visual inspection observations of Figs. 9 and 10. In respect to the other two methods, the Moroney technique is positioned second for the preference score (0.62), and the retinex model (0.46) is third. The psychovisual test and results are detailed in Sec. 5.

Let us now elaborate one of these images (for example, the one in Fig. 9) in their color version. In Fig. 12, we



Fig. 9 (a) Original image. (b) Our proposed method. (c) Moroney correction. (d) Retinex.

compare our results (we now take into account the saturation module of Sec. 2.4.2) with the Moroney correction and with the retinex approach in its Frankle-McCann²⁶ version. The strength of detail enhancement is observed in all three elaborated images. The retinex shows a color change that makes the result overenhanced and unnatural. Our algorithm achieves a good contrast enhancement (at both local and global scales) while affecting the colors in a more pleasing way. The Moroney correction is darker compared to the other two methods. This shows the effectiveness of our automated α parameter tuning and saturation preserving treatment. Comparisons have been also made between our method and the MSRC of Jobson *et al.*⁸ (not shown in this paper), and similar conclusions to the comparison with retinex results presented here can be drawn.

4 Conclusions

In this work, we presented a local contrast correction algorithm that allows for simultaneous shadow and highlight

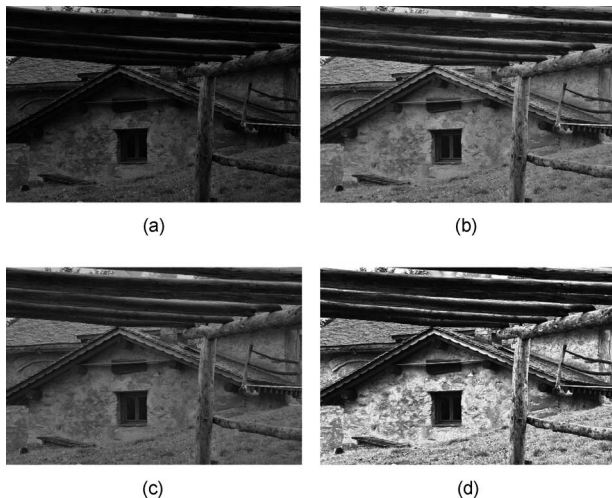


Fig. 10 (a) Original image. (b) Our proposed method. (c) Moroney correction. (d) Retinex.

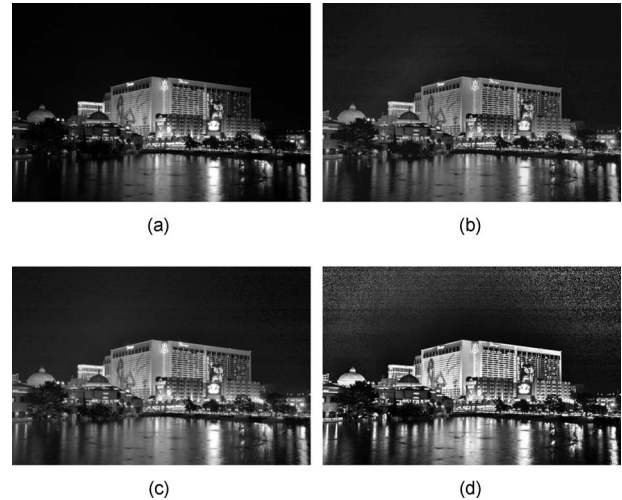


Fig. 11 (a) Original image (EME=25.09, H=5.86). (b) Our proposed method (EME=18.09, AMBE=18.89, H=6.01). (c) Moroney correction (EME=23.76, AMBE=23.86, H=6.58). (d) Retinex (EME=31.70, AMBE=48.58, H=7.61).

adjustments, starting from a simple pixel-wise gamma correction, automatically piloted by image statistics analysis. In order to prevent introduction of halo artifacts, an edge preserving filter, based on bilateral low-pass techniques, has been adopted. The proposed method, compared with other solutions well known in the literature, properly enhances the dynamic range in both low-light and high-light regions of an image while avoiding common quality loss due to halo artifacts, desaturation, and grayish appearance. The Mean Opinion Score test has been carried out to evaluate the performance of different contrast correction methods for the case of grayscale images. The highest score was obtained for our proposed algorithm. Our method has shown to be robust with respect to a heuristic choice of parameters. However, a further improvement could be achieved with an optimization procedure to estimate their values starting from a proper image database.

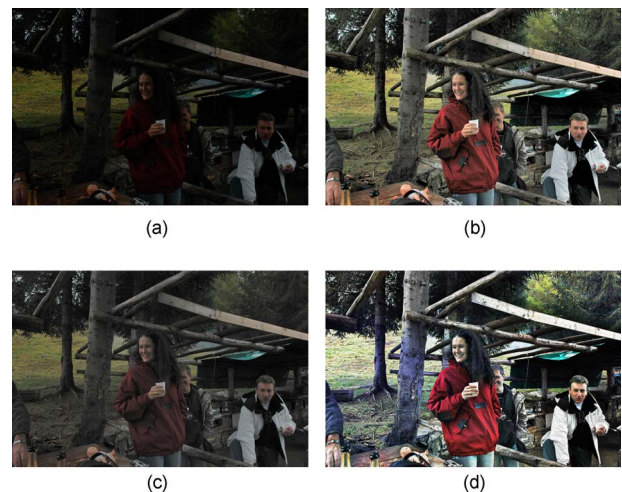


Fig. 12 (a) Original image. (b) Our proposed method. (c) Moroney correction. (d) Retinex.

Appendix

A psychovisual experiment (Mean Opinion Score) was performed using a paired comparison in which viewers were asked to select an image from a pair, based on their preference.³⁰ During the tests, the following algorithms were compared:

- Identity algorithm (the original scene)
- Our algorithm (LCC+clipping+saturation)
- Moroney⁴
- Retinex²⁶

1 Test Method

Ten badly exposed scenes (grayscale images) were used for the test. We used four different versions of each scene, one for each algorithm. On each trial of the experiment, subjects viewed a pair of images. A pair was formed by two versions of the same scene, and the subject was asked to indicate which image was the preferred one. Each version of a scene was compared with all the other versions of the same scene, for a total of 60 pairs (10 scenes \times 6 combinations). In all the experiments, the images were shown in a random order, different for each subject. During a preliminary test, each subject was implicitly trained about the kind of images he/she was going to evaluate.

2 Test Condition

To perform the psychovisual test, the images to be judged were shown on a web-based interface. We have adopted five 19-in CRT COMPAQ S9500 display monitors. All the monitors were calibrated (D65, gamma 2.2, luminance 100 cd/m²). Their resolution was 1600 \times 1200 pixels that correspond to 110 dpi (using 18 in as the physical diagonal of the screen, as indicated by the manufacturer). The refresh rate was 75 Hz. The ambient light levels (typical office illumination) were maintained constant between the different sessions. The distance between the observer and the monitors was about 60 cm (corresponding to about 46 pixels per deg of visual angle). All the original scenes utilized for the psychovisual tests were cropped and under-sampled to fit a 600 \times 600 pixel box.

3 Viewers

The panel of subjects involved in this study was recruited from the Computer Science Department. The subject pool consisted of 12 students inexperienced with image quality assessment. Subjects had normal or corrected-to-normal visual acuity. Each subject was individually briefed about the modality of the experiment in which he/she was involved. During the test, we evaluated a total of 720 pairs (12 viewers \times 10 scenes \times 6 combinations). The preference score is defined as the percentage of times an algorithm was preferred on the total number of (evaluated) pairs where it was present (10 scenes \times 12 viewers \times 3 combinations). The standard error of the mean (SEM) along the algorithm dimension was also estimated. The preference scores for each algorithm and the corresponding SEM are shown in Table 1.

Table 1 Mean Opinion Score experiment: Preference scores with standard error mean (SEM).

	Identity	Our algorithm	Moroney	Retinex
Preference score	0.1306	0.7944	0.6167	0.4583
SEM	± 0.0241	± 0.0259	± 0.0626	± 0.0452

References

1. W. Frei, "Image enhancement by histogram hyperbolization," *Comput. Graph. Image Process.* **6**, 286–294 (1977).
2. A. Mokrane, "A new image contrast enhancement technique based on a contrast discrimination model," *CVGIP: Graph. Models Image Process.* **54**, 171–180 (1992).
3. Y. Wang, Q. Chen, and B. Zhang, "Image enhancement based on equal area dualistic sub-image histogram equalization method," *IEEE Trans. Consum. Electron.* **45**, 68–75 (1999).
4. N. Moroney, "Local colour correction using nonlinear masking," in *IS&T/SID Eighth Color Imaging Conference*, Vol. 8, IS&T, pp. 108–111 (2000).
5. A. Stark, "Adaptive image contrast enhancement using generalizations of histogram equalization," *IEEE Trans. Image Process.* **9**, 889–896 (2000).
6. T. Arici, S. Dikbas, and Y. Altunbasak, "A histogram modification framework and its application for image contrast enhancement," *IEEE Trans. Image Process.* **18**, 1921–1935 (2009).
7. E. H. Land and J. J. McCann, "Lightness and retinex theory," *J. Opt. Soc. Am.* **61**, 1–11 (1971).
8. D. Jobson, Z. Rahman, and G. Woodell, "A multiscale retinex for bridging the gap between color images and the human observation of scenes," *IEEE Trans. Image Process.* **6**, 965–976 (1997).
9. Z. Rahman, D. Jobson, and G. Woodell, "Multiscale retinex for color image enhancement," in *Proc. Int. Conf. Image Processing*, vol. 3, pp. 1003–1006, IEEE, Piscataway, New Jersey (1996).
10. Z. Rahman, D. J. Jobson, and G. A. Woodell, "Retinex processing for automatic image enhancement," *J. Electron. Imaging* **13**, 100–110 (2004).
11. Z. Rahman, D. J. Jobson, G. A. Woodell, and G. D. Hines, "Image enhancement, image quality, and noise," in *Photonic Devices and Algorithms for Computing VII*, K. M. Iftakharuddin and A. A. S. Awwal, Eds., *Proc. SPIE* 5907, 164–178 (2005).
12. J. Starck, F. Murtagh, E. Candès, and D. Donoho, "Gray and color image contrast enhancement by the curvelet transform," *IEEE Trans. Image Process.* **12**, 706–716 (2003).
13. A. Rizzi, C. Gatta, and D. Marini, "A new algorithm for unsupervised global and local color correction," *Pattern Recogn. Lett.* **24**, 1663–1677 (2003).
14. M. D. Fairchild and G. M. Johnson, "Meet iCAM: A next-generation color appearance model," *IS&T/SID 10th Color Imaging Conference*, Scottsdale, Arizona, pp. 33–38 (2002).
15. K. Chiu, M. Herf, P. Shirley, S. Swamy, C. Wang, and K. Zimmerman, "Spatially nonuniform scaling functions for high contrast images," in *Proc. Graphics Interface'93*, pp. 245–254, Morgan Kaufmann (1993).
16. G. Larson, H. Rushmeier, and C. Piatko, "A visibility matching tone reproduction operator for high dynamic range scenes," *IEEE Trans. Vis. Comput. Graph.* **3**, 291–306 (1997).
17. J. Tumblin and G. Turk, "LCIS: a boundary hierarchy for detail preserving contrast reduction," in *SIGGRAPH 99*, pp. 83–90, ACM/Addison-Wesley, New York (1999).
18. S. Battiato, A. Castorina, and M. Mancuso, "High dynamic range imaging for digital still camera: an overview," *J. Electron. Imaging* **12**, 459–469 (2003).
19. L. Meylan and S. Süsstrunk, "High dynamic range image rendering with a Retinex-based adaptive filter," *IEEE Trans. Image Process.* **15**, 2820–2830 (2006).
20. F. Durand and J. Dorsey, "Fast bilateral filtering for the display of high-dynamic-range images," in *SIGGRAPH*, pp. 257–266, ACM/Addison-Wesley, New York (2002).
21. S. Pattanik, J. Ferwerda, M. Fairchild, and D. Greenberg, "A multi-scale model of adaptation and spatial visual for realistic image display," in *SIGGRAPH 98*, pp. 287–298, ACM/Addison-Wesley, New York (1998).
22. C. Tomasi and R. Manduchi, "Bilateral filtering for gray and color images," in *Proc. 1998 IEEE Int. Conf. Computer Vision*, pp. 836–846, IEEE, Piscataway, New Jersey (1998).
23. A. Capra, A. Castorina, S. Corchs, F. Gasparini, and R. Schettini, "Dynamic range optimization by local contrast correction and histo-

- gram image analysis," in *IEEE Int. Conf. Consumer Electronics, ICCE 2006*, pp. 309–310, IEEE, Piscataway, New Jersey (2006).
24. S. Paris and F. Durand, "A fast approximation of the bilateral filter using a signal processing approach," in *European Conf. Computer Vision (ECCV'06)*, A. Leonardis, H. Bishop, and A. Pinz, pp. 568–580, Springer, Berlin (2006).
 25. S. Sakaue, A. Tamura, M. Nakayama, and S. Maruno, "Adaptive gamma processing of the video cameras for the expansion of the dynamic range," *IEEE Trans. Consum. Electron.* **41**, 555–562 (1995).
 26. J. Frankle and J. McCann, "Method and apparatus for lightness imaging," U.S. Patent No. 4,384,336 (1983).
 27. Beghdadi A. and A. L. Négrate, "Contrast enhancement technique based on local detection of edges," *Comput. Vis. Graph. Image Process.* **46**, 162–174 (1989).
 28. S.-D. Chen and A. Ramli, "Minimum mean brightness error bi-histogram equalization in contrast enhancement," *IEEE Trans. Consum. Electron.* **49**, 1310–1319 (2003).
 29. S. Aghaian, K. Panetta, and A. Grigoryan, "Transform-based image enhancement algorithms with performance measure," *IEEE Trans. Image Process.* **10**, 367–382 (2001).
 30. P. Engeldrum, "Psychometric scaling: A toolkit for imaging systems development," Imcotek, Winchester, MA (2000).



Raimondo Schettini is an associate professor at the University of Milano-Bicocca (Italy). He is vice director of the Department of Informatics, Systems, and Communication and head of the Imaging and Vision Lab. He has been associated with the Italian National Research Council (CNR) since 1987. He has been team leader on several research projects and has published more than 190 refereed papers on image processing, analysis, and reproduction and on image content-based indexing and retrieval.

He is an associated editor of the *Pattern Recognition Journal*. He was a co-guest editor of three special issues about Internet imaging (*Journal of Electronic Imaging*, 2002), color image processing and analysis (*Pattern Recognition Letters*, 2003), and color for image indexing and retrieval (*Computer Vision and Image Understanding*, 2004). He was a member of the CIE TC 8/3 and chairman of the 1st Workshop on Image and Video Content-Based Retrieval (1998); the First European Conference on Color in Graphics, Imaging and Vision (2002); the EI Internet Imaging Conferences (2000–2006); the EI Multimedia Content Access: Algorithms and Systems 2007 Conference (2007, 2009, 2010); and the Computational Color Imaging Workshop (2007, 2009, 2011).



Francesca Gasparini received her degree (Laurea) in nuclear engineering from the Polytechnic of Milan in 1997 and her PhD in science and technology in nuclear power plants from the Polytechnic of Milan in 2000. Since 2001, she has been a fellow at the ITC Imaging and Vision Laboratory of the Italian National Research Council. Gasparini is currently an assistant professor at the Dipartimento di Informatica, Sistemistica e Comunicazione (DISCo), University of Milano-Bicocca, where her research focuses on image and video enhancement, face detection, and image quality assessment.



ity assessment, and visual attention mechanisms applied to image processing.



Fabrizio Marini received his degree in computer science from the University of Milano-Bicocca (Italy) in 2007. He is currently a PhD student in computer science at the Dipartimento di Informatica, Sistemistica e Comunicazione (DISCo) of the University of Milano-Bicocca. The main topics of his current research concern image quality assessment and imaging device characterization.



ents and papers in these R&D fields.

Alessandro Capra received his electronic engineering degree from the University of Palermo in 1998. Since 1999, he has worked at STMicroelectronics. His main activities have been related to research innovative architectures and algorithms for digital still camera and mobile imaging applications. He is currently in charge of a team developing next-generation image processing algorithms and systems for mobile cameras. He is author of many patents and papers in these R&D fields.



Alfio Castorina received his degree in computer science in 2000 at the University of Catania. Since 2000, he has been working at STMicroelectronics in the Advanced System Technology (AST) Catania Lab as a system engineer. He is author of several papers and patents in the image and video processing field.